

# Skeletal manifestations in a streptozotocin-induced C57BL/6 model of Type 1 diabetes

Jennifer M. Hatch, Dyann M. Segvich, Rachel Kohler, Joseph M. Wallace\*

Department of Biomedical Engineering, Indiana University-Purdue University at Indianapolis, Indianapolis, IN, USA

## ARTICLE INFO

### Keywords:

Bone  
Hyperglycemia  
HbA1c  
Mechanics  
GTT  
ITT

## ABSTRACT

Diabetes Mellitus is a metabolic disease which profoundly affects many organ systems in the body, including the skeleton. As is often the case with biology, there are inherent differences between the sexes when considering skeletal development and disease progression and outcome. Therefore, the aim of this study was to develop a protocol to reliably induce diabetes in both sexes of the C57BL/6 mouse utilizing streptozotocin (STZ) and to characterize the resulting bone phenotype. We hypothesized that destruction of the  $\beta$ -cells in the pancreatic islet by STZ would result in a diabetic state with downstream skeletal manifestations. Beginning at 8 weeks of age, mice were injected for 5 consecutive days with STZ (65 mg/kg males, 90 mg/kg females) dissolved in a citrate buffer. The diabetic state of the mice was monitored for 5 weeks to ensure persistent hyperglycemia and mice were euthanized at 15 weeks of age. Diabetes was confirmed through blood glucose monitoring, glucose and insulin tolerance testing, HbA1c measurement, and histological staining of the pancreas. The resulting bone phenotype was characterized using microcomputed tomography to assess bone structure, and whole bone mechanical testing to assess bone functional integrity. Mice from both sexes experienced loss of  $\beta$ -cell mass and increased glycation of hemoglobin, as well as reduced trabecular thickness and trabecular tissues mineral density (TMD), and reduced cortical thickness and cortical bone area fraction. In female mice the change area fraction was driven by a reduction in overall bone size while in male mice, the change was driven by increased marrow area. Males also experienced reduced cortical TMD. Mechanical bending tests of the tibiae showed significant results in females with a reduction in yield force and ultimate force driving lower work to yield and total work and a roughly 40 % reduction of stiffness. When tissue level parameters were estimated using beam theory, there was a significant reduction in yield and ultimate stresses as well as elastic modulus. The previously reported mechanistic similarity in the action of STZ on murine animals, as well as the ease of STZ administration via IP injection make this model a strong candidate for future exploration of osteoporotic bone disease, Diabetes Mellitus, and the link between estrogen and glucose sensitivity.

## 1. Introduction

The World Health Organization (WHO) estimates that in 2016, 8.5 % of adults worldwide suffered from Diabetes Mellitus, an increase from 4.7 % in 1980 (W. H. Organization, 2016). This level is expected to rise to roughly 7.7 % by 2030 (Shaw et al., 2009). Type I Diabetes Mellitus (T1D) is often diagnosed in childhood and is characterized by an inability to produce insulin endogenously. As a group, T1D patients exhibit reduced bone mass when compared to age matched peers and while this loss is relatively small (<10 % or within one standard deviation) it occurs during peak bone formation years, prohibiting patients from reaching ideal peak bone mass during adolescence (Bouillon, 1991;

Hough et al., 2016). Further, diabetic patients experience lower bone turnover rates, impaired bone healing, lower bone density and are more likely to experience falls and to suffer from bone fractures due to underlying skeletal deficiencies (Report, 2020; Sundararaghavan et al., 2017; Starup-Linde et al., 2019).

The streptozotocin (STZ) mouse model of diabetes uses STZ, chemotherapeutic agent used clinically to treat pancreatic cancer, to ablate the pancreatic  $\beta$ -islet cells responsible for producing insulin in response to elevated blood glucose. In humans, the onset of T1D affects the bone through multiple pathways; insulin deficiency drives a reduction of the viable pool of osteoblast progenitors through insufficient transcription of Runx-2 (Fowlkes et al., 2008) and reduced production of

\* Corresponding author at: 723 W. Michigan St., SL 220, Indianapolis, IN 46202, USA.  
E-mail address: [jmwalla@iupui.edu](mailto:jmwalla@iupui.edu) (J.M. Wallace).

<https://doi.org/10.1016/j.bonr.2022.101609>

Received 25 June 2022; Received in revised form 27 July 2022; Accepted 30 July 2022

Available online 1 August 2022

2352-1872/© 2022 The Authors. Published by Elsevier Inc. This is an open access article under the CC BY-NC-ND license (<http://creativecommons.org/licenses/by-nc-nd/4.0/>).

new collagen by osteoblasts through decreased binding with receptors for IGF-1 and insulin receptors (Palta et al., 2014; Bouillon, 1992); the downregulation of the Wnt/ $\beta$ -catenin pathway due to increased secretion of sclerostin by osteocytes (Hie et al., 2011); decreased osteocalcin production by osteoblasts (Inaba et al., 1995); increased circulation of inflammatory cytokines (Jeffcoate et al., 2005; Jin et al., 2013); increased levels of RANKL leading to higher numbers of osteoclasts (Zhou et al., 2006; Tsentidis et al., 2016); and accumulation of advanced glycation end product (AGEs) through non-enzymatic glycosylation of collagen causing apoptosis of mesenchymal stem cells further reducing the pool of potential osteoprogenitors and decreasing the mineralization of new bone (Santana et al., 2003; Yamagishi et al., 2005). STZ models of diabetes in rats and mice exhibit many of the same chemical markers: reduced Runx-2 transcription (Fowlkes et al., 2008; Hie et al., 2011; Lu et al., 2003); downregulation in the Wnt/ $\beta$ -catenin pathway (Portal-Nunez et al., 2010); reduced expression of IGF-1 and insulin receptors (Bouillon, 1992; Zhao et al., 2013); increased production of inflammatory cytokines (Niu et al., 2016); altered sclerostin production and increased levels of RANKL (Bortolin et al., 2015); and decreased levels of osteocalcin (Hie et al., 2011). The mechanistic commonalities of STZ-induced diabetes with human T1D along with the high specificity of toxicity to the cells of the pancreatic  $\beta$ -islet, the ability to control the timeline of diabetic onset, and the high success rate of induction (Nahdi et al., 2017) indicate this model to be a powerful tool for the study of diabetes.

In theory, the use of the STZ mouse model is well-established though many protocols of induction exist. STZ use is reported at varying dosages (55–275 mg/kg), for varying lengths of time (injections for 1–5 days), and through various delivery methods, and the sensitivity of an individual mouse to STZ is strain, sex, and breeder dependent (Chandramouli et al., 2018; Gurley et al., 2006; Hayashi et al., 2006; Leiter, 1985; Nakamura et al., 1984; Bell et al., 1994; Cortright et al., 1996; Le May et al., 2006). Interactions between the cells of the pancreas and estrogen make it difficult to induce diabetes in female mice using STZ, with male mice experiencing more severe disease phenotypes at lower doses (Cortright et al., 1996; Le May et al., 2006). In the study of diabetic bone, male Lewis rats have often been used, with mixed reports on reduced tibial length and reduced torsional strength and increase in stiffness, while male Wistar rats have shown a reduction in femoral strength when tested in three-point bending (Cortright et al., 1996; Einhorn et al., 1988; Horcajada-Molteni et al., 2001). Male Balb-C mice treated with STZ have shown significantly reduced trabecular bone volume fraction (BV/TV), volumetric bone mineral density (BMD), and trabecular thickness in tibiae after STZ treatment, although this was not accompanied by a significant change in tibial length (Bortolin and McCabe, 2007). CD-1 mice (the sex of which was not reported) treated with STZ had reduced bone formation through quantitative histomorphometric analysis (Lu et al., 2003; Motyl and McCabe, 2009). Male C57BL/6 mice were studied by Hamada et al. in 2007 after 12 weeks of STZ treatment, showing a decreased bone volume fraction, and reduced bone formation (Hamada et al., 2007). Recently, STZ induced male and female C57BL/6J mice have been shown to have reduced bone healing capabilities, with female mice expressing increased amounts of inflammatory marker IGF-1 and both sexes presenting with a lower BV/TV in the trabecular bone of the tibiae (Cignachi et al., 2020).

The previously mentioned sequelae of cellular changes in diabetes result in the alteration of trabecular microarchitecture, reduced cortical bone volume, and detrimental impacts on bone mechanical properties (Einhorn et al., 1988; Motyl and McCabe, 2009; Ni et al., 2019; Weinberg et al., 2014). However, these studies failed to consider the possibility that sex-specific skeletal impacts might exist, a crucial consideration given that diabetes is equally prevalent among aging human men and women and that, clinically, women have been observed to have worse bone-health related outcomes (Schwartz et al., 2002). The aim of this study was to develop a protocol to reliably induce diabetes in mice from both sexes, and to characterize the resulting disease

phenotype with a focus on skeletal manifestations and the potential downstream effects on the mechanical performance of the bone. It was hypothesized that once a diabetic state was established, elevated blood glucose would drive quality-based changes and altered architecture in the bones of mice from both sexes, resulting in mechanical deficits.

## 2. Materials and methods

### 2.1. Mouse model

Male and female C57BL/6 mice were purchased from Envigo labs (Indianapolis, IN) at 7 weeks of age and allowed 1 week in our facility to acclimate prior to the initiation of the study. Mice were grouped into weight-matched treatment groups (Control (ctrl) or Treatment (STZ)) within each sex (n = 15 per group). Mice were administered either STZ dissolved in a 50 mM citrate buffer vehicle control or vehicle alone via intraperitoneal injection for 5 consecutive days starting at 8 weeks of age (females: 90 mg/kg, males: 65 mg/kg). Mice were sacrificed at 15 weeks of age via cardiac exsanguination, through which up to 1 mL of blood was collected, followed by cervical dislocation. Bones were wrapped in phosphate-buffered saline (PBS)-soaked gauze and stored at  $-20^{\circ}\text{C}$ . Animal experiments were approved through the IACUC at Indiana University-Purdue University Indianapolis (protocol # SC309R), and carried out with deference to the guidelines set forth by the National Research Council in the *Guide for the Care and Use of Laboratory Animals (Guide for the Care and Use of Laboratory Animals, 2011)*.

### 2.2. Blood glucose measurements

Non-fasting blood glucose measurements were made in all mice prior to the first STZ injection. Ctrl mice were monitored for two consecutive weeks while STZ mice were monitored for four consecutive weeks to confirm BG of all control mice was  $<300$  mg/dL and BG of all STZ mice was  $>300$  mg/dL. The BG of all mice were measured at sacrifice. Blood was collected from the tip of the tail and measured on an Alpkatrak 2 glucometer using the mouse setting adjustment prescribed by the manufacturer (Zoetis Products, Chicago Heights, IL).

### 2.3. Glucose and insulin tolerance testing

Mice were subjected to either glucose tolerance testing (GTT, n = 7 per group) or insulin tolerance testing (ITT, n = 8 per group) at 15 weeks of age, prior to the study endpoint. Mice in the GTT group were fasted overnight and injected subcutaneously with a bolus of glucose (2 g/kg) at time = 0. Blood glucose measurements were made at 0, 10, 20, 30, 60, and 90-minute timepoints. Mice in the ITT group were fasted for 2 h prior to testing and injected subcutaneously with a bolus of insulin (0.75 U/kg) at time = 0. Blood glucose measurements were made at 15-minute intervals over the course of 1 h. Data are reported as area under the curve based on averaged values for each group at each timepoint.

### 2.4. Pancreatic analysis

Pancreata from 5 mice in each group were harvested and weighed, then fixed in 10 % formalin for 6 h. Specimen were dehydrated through a graded ethanol sequence, cleared with two changes of xylenes, and submerged through four changes of melted paraffin ( $\sim 60^{\circ}\text{C}$ ). Pancreata were then embedded in paraffin, allowed to harden, and sectioned using a rotary microtome. Sections were flattened on a heated water bath, floated onto microscope slides, then dried. Each slide was incubated with anti-insulin (C27C9) rabbit monoclonal antibodies (Cell Signaling Technology, Danvers, MA) overnight at  $4^{\circ}\text{C}$ . Insulin was visualized with anti-rabbit ImmPRESS reagent and NovaRed substrate kit; hematoxylin was used to counterstain the tissue. From each pancreas, 5 sections separated by at least 50  $\mu\text{m}$  were analyzed using Zen Blue software

(Zeiss, Oberkochen, Germany). The insulin-positive area in pixels was divided by the total pancreas area in pixels and expressed as a percentage. Embedding and sectioning was performed by the Histology Core in the Indiana Center for Musculoskeletal Health at Indiana University School of Medicine. Staining and measurements were performed by the Islet and Physiology Core in the Center for Diabetes and Metabolic Diseases at Indiana University School of Medicine.

### 2.5. HbA1c analysis

0.5–1 mL of blood was collected via cardiac exsanguination and stored in EDTA coated tubes. HbA1c was measured using a latex agglutination inhibition assay. Total hemoglobin was determined by conversion to alkaline haematin in non-ionic detergent. The reported values are the ratio of the glycated hemoglobin to the total hemoglobin. Measures were performed by the Translation Core in the Center for Diabetes and Metabolic Diseases at Indiana University School of Medicine on a Daytona+ clinical chemistry analyzer (Randox Laboratories, Crumlin, United Kingdom).

### 2.6. Microcomputed tomography ( $\mu$ CT)

Right and Left tibiae were scanned three at a time, through a 0.5 mm aluminum filter ( $V = 60$  kV,  $I = 167$   $\mu$ A) at a 9.8  $\mu$ m/voxel resolution on a Skyscan 1172 (Bruker, Kontich, Belgium) (Kohler et al., 2021). Scans were performed at intervals of 0.7 degrees, averaging two frames at each increment. Scans of hydroxyapatite phantoms (0.25 and 0.75 g/cm<sup>3</sup> CaHA) were used to calibrate bone mineral density. Image reconstruction was performed in NRecon software (Bruker, Kontich, Belgium) and images were rotated in DataViewer (Bruker, Kontich, Belgium) to ensure consistent orientation. To analyze geometric properties, 1-mm trabecular regions of interest beginning just distal to the proximal tibial growth plate were segmented from the surrounding cortical shell in CTan software. Bone was segmented from non-bone using a grayscale threshold of 70 to delineate soft tissue and artifact from bone. Trabecular bone was segmented from cortical bone using the contouring threshold program native to CTan software. CTan was then used to measure bone volume fraction (BV/TV), trabecular number (Tb. N.), trabecular separation (Tb. Sp.), trabecular thickness (Tb. Th.), and tissue mineral density (TMD). A 1-mm cortical region of interest at the tibial mid-diaphysis of each bone was chosen. The geometry of each section was evaluated in a custom MATLAB (MathWorks, Natick, MA) script to find total cross-sectional area (TA), bone area (BA), marrow area (MA), bone area fraction (BA/TA), cortical thickness (Ct. Th.), moments of inertia along the minor (I<sub>min</sub>) and major axes (I<sub>max</sub>), and cortical TMD.

### 2.7. Mechanical testing

Left tibiae were tested to failure in a 4-point bending configuration with a 9 mm support span and a 3 mm loading span (TA Electroforce 5500). Displacement was applied monotonically in the medial-lateral direction at 0.025 mm/s (medial surface in tension). Bones were kept hydrated with PBS throughout the test. Force and displacement values were recorded. Analysis was performed in MATLAB (MathWorks, Natick, MA) to construct a force-displacement curve which was normalized with  $\mu$ CT data and standard engineering bending equations for four-point bending to produce a stress-strain curve. Yield was identified using the 0.2 % strain offset method after which the yield point was mapped back to the force/displacement domain. Working in the force/displacement domain, yield force, maximum force, displacement at yield, post-yield displacement, and total displacement were determined. Stiffness was taken from the linear slope in the elastic region and work to yield, post-yield work, and total work were calculated from the area underneath the curve. In the stress/strain domain, yield stress, ultimate stress, strain to yield, and total strain were identified. The slope of the stress-strain curve in the elastic region was taken as the elastic

modulus, the area under the elastic region of the curve was taken as the resilience, and the area under the entire curve was taken as toughness (Wallace, 2019).

### 2.8. Bone fluorescent advanced glycation end product (fAGE) analysis

After mechanical testing, 5 samples from each group were randomly selected for quantification of bone AGEs. The ends of the broken left tibiae were removed, and marrow was flushed from the marrow cavity. Bones were demineralized for 30 min in Immunocal™ Decalcifier solution (StatLab, McKinney, TX) until clear and pliable. Demineralized bones were rinsed with water, weighed, and dried overnight in an oven at 37 °C. Samples were transferred to glass hydrolysis tubes and digested with 100  $\mu$ L 6 M HCL/mg at 110 °C for 20 h. Samples were cooled, diluted with water, and tested on a Cytation 3 plate reader (Biotek, Winooski, VT) with fluorescence capabilities at 360 nm excitation and 460 nm emission. Samples were tested against a quinine standard and values were normalized to collagen content using a colorimetric assay kit for hydroxyproline as a marker for collagen (BioVision Inc., Milpitas, CA).

### 2.9. Statistical analysis

Statistical analyses were performed in Prism (GraphPad v. 9, San Diego, CA). All data within each sex were evaluated via two-tailed, unpaired Student t-tests (with  $p < 0.05$  set as the threshold for statistical significance). Where data points failed to fall within a normal distribution, a Mann-Whitney rank sum test was performed. The area under the curve (AUC) function in Prism was utilized to calculate AUC for each GTT and ITT test. These values were then evaluated via t-test. All data are reported as mean  $\pm$  standard deviation unless otherwise noted.

## 3. Results

### 3.1. STZ treatment effectively led to hyperglycemia in male and female mice

For this study, a threshold of 300 mg/dL blood glucose was set to differentiate between diabetic and healthy mice. Prior to induction, the blood glucose of all mice was confirmed to be below this threshold. One week following the final STZ injection, 13 of the 15 female mice and 14 of the 15 male mice had measured blood glucose above the diabetic threshold. Two weeks following the final injection 100 % of mice had crossed the diabetic threshold. Glucose was tracked for two consecutive weeks in the control mice to verify that no mice became spontaneously diabetic, and for four consecutive weeks in STZ mice to ensure persistent hyperglycemia. Blood Glucose was again measured at sacrifice, with 100 % of the diabetic mice measuring over the 300 mg/dL threshold, and all control mice measuring below the 300 mg/dL threshold.

### 3.2. Ablation of $\beta$ -cells by STZ leads to increased HbA1c, reduced mass and reduced tibial length

The percent change in body mass over the course of the study was significantly different in STZ-treated mice versus control mice ( $p < 0.0001$  for both sexes). On average control mice saw an increase in body mass of 14.6 % at sacrifice over initial mass while STZ mice decreased by 2.5 % (Fig. 1, A). Final tibial length was significantly decreased in female STZ-treated mice versus control ( $p = 0.0039$  Fig. 1, B). HbA1c was used as a measure of the average percent of glycated hemoglobin in the blood (Fig. 1, C). In both male and female STZ-treated mice, HbA1c was nearly doubled versus control mice ( $p < 0.0001$  in both cases). Immunohistochemical analysis of sections taken from the pancreata showed a significant decrease in percent  $\beta$ -cell area in STZ-treated females versus control ( $p < 0.0001$ ). Although it trended downward, this decrease failed to reach significance in male mice.

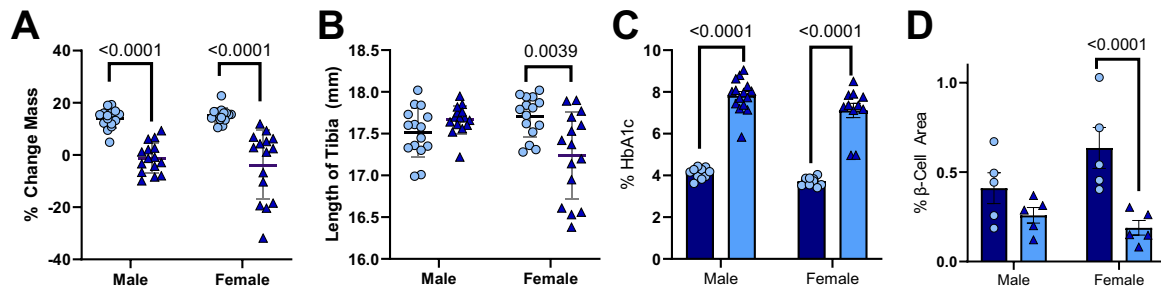


**Fig. 1.** Differences in mass, tibial length and HbA1c following reduction of  $\beta$ -cell area. A. STZ-treated mice gained significantly less mass over the duration of the study in both sexes. Percent change of mass was calculated as the final mass at 15 weeks of age divided by the initial mass at 8 weeks of age, multiplied by 100. B. Tibial length in STZ-treated females was shorter compared with control mice while no difference was noted in males. C. STZ-treated mice had significantly higher levels of glycated hemoglobin in the blood compared to control mice. D. STZ-treated females had significantly lower  $\beta$ -cell population in the pancreas compared to healthy mice. Data presented as mean  $\pm$  SD.

**3.3. STZ-treated mice lose ability to metabolize glucose**

To evaluate glucose tolerance and assess  $\beta$ -cell function, a glucose tolerance test (GTT) was performed three days prior to sacrifice, 6 weeks after the last STZ injection (Fig. 2, A). Mice were fasted for 12 h before testing. At time = 0 female mice in both the control and treatment groups had BG levels lower than the 300 mg/dL threshold used to classify hyperglycemia. In contrast, while male mice in the control group were within the healthy BG range, STZ-treated males had elevated BG even after the 12-hour fast. Mice from both sexes treated with STZ had impaired glucose tolerance. In control animals, blood glucose spiked and

peaked within the first 10 min of observation. The glucose in the diabetic mice continued to climb, peaking around 30 min for the males and around 1 h for the females. Control mice rapidly returned to the fasting blood glucose level, fully recovering within the first hour. Treated mice did not begin to process the glucose as quickly, and never returned to their fasting blood glucose levels. The area under the curve was calculated for each group, showing a significant elevation in the STZ treated mice from both sexes ( $p < 0.0001$ , Fig. 2, C).

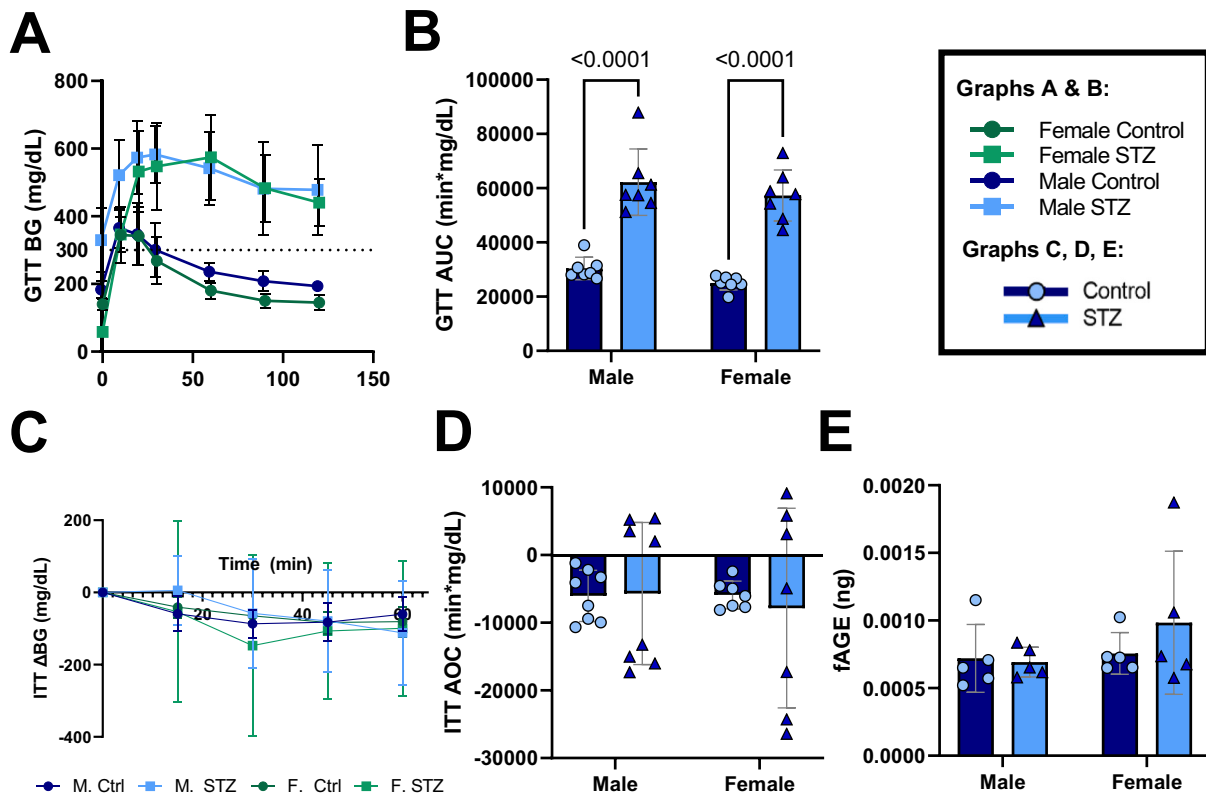


**Fig. 2.** STZ-treated mice lack endogenous insulin yet retain the ability to utilize exogenous insulin. A. Control mice responded to a bolus glucose injection within 10 min, returning close to pre-injection levels after 1 h. STZ males showed no signs of metabolizing glucose until the 45-min mark, while STZ females did not begin to metabolize glucose within the first hour after injection. STZ mice did not recover to pre-injection BG levels during the time-course of the observation. B. Comparison of the areas under the curves generated from GTT data indicate a significant impairment in the ability of STZ-treated mice to process the injected glucose. C. Insulin tolerance test results normalized to the BG level at time = 0 show that mice in all groups responded similarly to injection of exogenous insulin. D. Comparison of the areas over the curves generated from ITT data show no significant change in the ability of STZ-treated mice to process injected insulin. E. There was no significant difference measured fAGEs in the bones of STZ treated mice versus control. Data presented as mean  $\pm$  SD.

### 3.4. STZ-treated mice retain the ability to process insulin

Glucose level of the control animals from both sexes began to decrease within the first time-segment after insulin injection, while the diabetic animals experienced a small spike in blood glucose 15 min post injection. Between 15 and 30 min, blood glucose of the diabetic animals began to drop. By the end of the hour, blood glucose of the diabetic animals was lower than pre-injection, although within the period of observation, blood glucose never dropped low enough to bring the mice out of a hyperglycemic state (Fig. 2, B). When the BG measurements at each time point were normalized to the BG at  $t = 0$ , there was no difference between the response of the control mice and the STZ mice to the exogenous insulin, indicating that STZ treated mice retain the ability to process exogenous insulin (Fig. 2, D).

### 3.5. fAGEs were not elevated in bone from STZ-treated mice

Tibiae, with the ends and marrow removed, were digested and processed for fAGE content. fAGEs were evaluated as a metric of the prevalence of non-enzymatic glycation events within the bone tissue. There were no significant differences in the levels of fluorescence measured in STZ-treated mice from either sex (Fig. 2, E).

### 3.6. Effects of STZ-treatment on bone morphology

STZ-treated mice from both sexes had lower TMD and trabecular thickness compared with their control counterparts (Table 1). No other trabecular properties differed in either sex. Analysis of the cortical bone at the tibial mid-diaphysis showed that STZ-treated males had enlarged marrow area which contributed to a significantly lower bone area fraction (Table 2). STZ significantly increased cortical TMD in male mice. STZ-treated females had significantly lower total area and bone area at the mid-diaphysis of the tibia resulting in a significantly lower bone area fraction. STZ-treated females also had lower principal moments of inertia compared to control females.

### 3.7. STZ-treatment alters mechanical performance of bones

At the whole bone level, there were no significant mechanical difference in STZ-treated males versus controls (Fig. 3, A; Table 3). Bones from STZ-females yielded and broke at forces that were, on average, 75 % lower than forces noted in control bones. This reduction in yield force led to a reduction in the amount of work needed to reach yield and maximum force. There was also a 41 % reduction in the stiffness in STZ-treated female bones.

At the tissue level, estimations of yield stress, ultimate stress, and elastic modulus were decreased in STZ-treated female versus controls (Fig. 3B; Table 4). There were no significant tissue level changes in STZ-treated male mice.

## 4. Discussion

STZ has been used for over 30 years as a means of destroying

pancreatic  $\beta$ -cells to induce a diabetic state in animal models (Junod et al., 1967). In the pancreas, STZ competes with glucose to enter the  $\beta$ -cell through the Glut2 complex. This specificity is a key aspect of the effectiveness of STZ. Once inside the cell, the methyl nitrosourea portion of the STZ alkylates DNA, breaking it into fragments. This activates Poly ADP-ribose synthetase to repair the DNA, which in turn depletes the NAD<sup>+</sup> supply. NAD<sup>+</sup> is crucial to the cellular production of ATP and the lowered ATP production results in the formation of hydrogen peroxide and hydroxyl radicals causing oxidative stress, after which cell death by both necrosis and apoptosis has been observed (Nahdi et al., 2017). Estrogen receptor alpha (ER- $\alpha$ ) presents abundantly on the surface of  $\beta$ -islet cells in females, creating the opportunity for estradiol to intervene in the destruction of cells by STZ by preserving the ability of the mitochondria to produce ATP and by promoting healthy protein production in the endoplasmic reticulum (ER) (Gupte et al., 2015). Few STZ studies use female models given the known difficulty in consistently establishing a diabetic state in this sex. In our prior attempts, male mice consistently and reliably became diabetic (blood glucose >300 mg/dL) after five daily injections of 45 mg/kg STZ. At that same dose, female mice did not become diabetic even when the initial 5-day treatment period was followed by a single booster shot of an additional 45 mg/kg one week after the first round of injections was completed. A pilot study assessed induction with varying doses of STZ. At 60 mg/kg, 50 % of female mice became diabetic. At 75 mg/kg, 83 % of mice became diabetic. At 90 mg/kg 100 % of mice became diabetic. During that study, 80 % of females and 86 % of males became consistently hyperglycemic one week following the final injection. By two weeks, 100 % of treated animals crossed the diabetic threshold. This informed the differential dosing used in the current study. As there was no factor by which to normalize male data to female data given the difference in STZ dosing, the sexes were considered separately for statistical evaluation. While using a differential dose allowed study of both sexes, the absence of a factor by which to normalize the severity of diabetes to the dose different between sexes is a limitation that prevents direct comparison of results from male and female mice.

Although histological examination of the pancreatic tissue indicated that  $\beta$ -cells were not completely absent, it is unclear if this is due to failure to completely destroy the  $\beta$ -cell population or if some cells regenerated during the 7 weeks following disease initiation. The decrease in %  $\beta$ -cell area observed in both sexes after STZ treatment paralleled the measured hyperglycemia in all STZ-treated mice over the duration of the study (BG > 300 mg/dL). Taken together, this indicates that STZ was the direct driver of the disease phenotype. Prior to euthanasia, all mice underwent either glucose or insulin tolerance testing to quantify the ability of the mice to produce and respond to insulin. GTT showed that STZ-treated mice were unable to modulate injected glucose, taking longer to reduce BG levels and doing so with less efficiency than control mice. Insulin production was compromised in the treated mice. However, when insulin was given to diabetic and control mice after a two hour fast, all groups responded similarly, reducing BG levels by comparable amounts at all timepoints. This finding suggests that while STZ-treated mice lost the ability to produce insulin endogenously, the ability to utilize insulin was not affected. Hyperglycemia resulting from a

**Table 1**  
Properties of trabecular bone microarchitecture from microcomputed tomography.

Trabecular bone properties	Male		p-Value	Female		p-Value
	Control (n = 15)	STZ (n = 15)		Control (n = 15)	STZ (n = 15)	
BV/TV (%)	14.70 ± 2.54	13.66 ± 1.89	0.141109	11.46 ± 1.73	10.87 ± 1.13	0.400065
Tb. Th. (mm)	0.0577 ± 0.0015	0.0551 ± 0.0025	<b>0.025616</b>	0.0616 ± 0.0021	0.0553 ± 0.0051	<b>&lt;0.000001</b>
Tb. N. (1/mm)	2.55 ± 0.46	2.48 ± 0.32	0.558661	1.86 ± 0.28	1.98 ± 0.20	0.352643
Tb. Sp. (mm)	0.19 ± 0.01	0.19 ± 0.01	0.423911	0.27 ± 0.04	0.26 ± 0.03	0.190540
TMD (g/cm <sup>3</sup> )	0.75 ± 0.01	0.73 ± 0.02	<b>0.008610</b>	0.77 ± 0.02	0.75 ± 0.03	<b>0.004614</b>

Values in bold denote significance.

**Table 2**  
Properties of cortical bone from microcomputed tomography.

Cortical bone properties	Male		p-Value	Female		p-Value
	Control	STZ		Control	STZ	
	(n = 15)	(n = 15)		(n = 15)	(n = 15)	
TA (mm <sup>2</sup> )	1.14 ± 0.10	1.19 ± 0.15	0.623594	1.04 ± 0.10	0.95 ± 0.11	<b>0.001187</b>
BA (mm <sup>2</sup> )	0.69 ± 0.06	0.67 ± 0.06	0.285441	0.65 ± 0.05	0.54 ± 0.06	<b>0.000009</b>
MA (mm <sup>2</sup> )	0.45 ± 0.04	0.52 ± 0.10	<b>0.004266</b>	0.38 ± 0.05	0.41 ± 0.08	0.187268
BA/TA (%)	60.87 ± 1.26	56.51 ± 3.50	<b>0.000348</b>	63.34 ± 1.90	57.06 ± 4.67	<b>&lt;0.000001</b>
Ct. Th. (mm <sup>2</sup> )	0.22 ± 0.01	0.25 ± 0.17	0.407012	0.22 ± 0.01	0.19 ± 0.02	0.251839
Imax (mm <sup>4</sup> )	0.12 ± 0.04	0.12 ± 0.05	0.838135	0.09 ± 0.04	0.07 ± 0.03	<b>0.000478</b>
Imin (mm <sup>4</sup> )	0.08 ± 0.01	0.08 ± 0.01	0.610319	0.07 ± 0.01	0.05 ± 0.01	<b>0.000439</b>
Ct. TMD (g/cm <sup>3</sup> )	1.32 ± 0.01	1.40 ± 0.07	<b>&lt;0.000001</b>	1.37 ± 0.07	1.40 ± 0.05	0.067496

Values in bold denote significance.

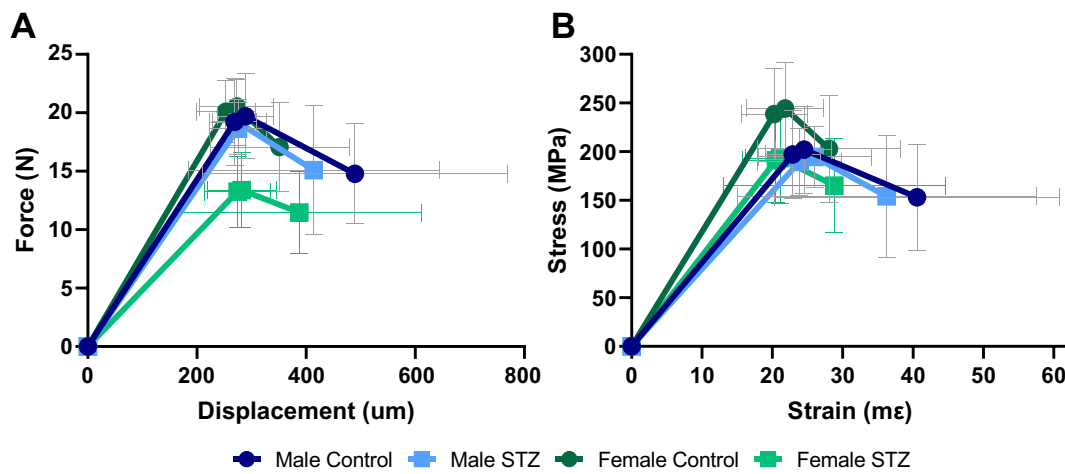


**Fig. 3.** A. Schematic Representations of Mechanical Data. Bones from STZ-treated female displayed lower yield and ultimate form versus those from control animals leading to reductions in work to yield and total work. B. Control bones withstood higher stresses than bones from STZ-treated mice. Data presented as mean ± SD, n = 15.

**Table 3**  
Structural-level mechanical data from 4-pt bending tests.

Force-displacement data	Male		p-Value	Female		p-Value
	Control	STZ		Control	STZ	
	(n = 15)	(n = 15)		(n = 15)	(n = 15)	
Yield force (N)	19.22 ± 3.72	18.66 ± 2.26	0.609501	20.10 ± 2.68	13.25 ± 3.05	<b>&lt;0.000001</b>
Ultimate force (N)	19.7 ± 3.52	19.18 ± 1.89	0.619420	20.54 ± 2.23	13.39 ± 3.09	<b>&lt;0.000001</b>
Displacement to yield (µm)	268.91 ± 41.26	275.37 ± 51.40	0.736219	253.07 ± 53.44	274.36 ± 61.08	0.269519
Post-yield displacement (µm)	220.67 ± 246.66	138.8 ± 234.76	0.228618	98.33 ± 98.42	113.6 ± 206.24	0.350524
Total displacement (µm)	489.58 ± 270.72	414.17 ± 221.75	0.682674	351.41 ± 123	387.96 ± 215.66	0.806334
Work to yield (mJ)	2.81 ± 0.78	2.77 ± 0.75	0.866746	2.75 ± 0.62	2.00 ± 0.67	<b>0.004953</b>
Post-yield work (mJ)	3.4 ± 3.47	1.6 ± 2.04	0.249556	1.65 ± 1.43	1.37 ± 2.36	0.61279
Total work (mJ)	6.21 ± 3.91	4.37 ± 1.86	0.412376	4.4 ± 1.65	3.37 ± 2.57	<b>0.029496</b>
Stiffness (N/mm)	78.19 ± 14.52	74.15 ± 12.15	0.482656	90.54 ± 21.53	53.65 ± 12.53	<b>&lt;0.000001</b>

Values in bold denote significance.

reduction in the number and health of the β-cells, separate from loss of the ability to process insulin, is a hallmark of T1D in humans (Ndisang et al., 2017). Patients with T2D also experience a reduction in the ability of the β-cells to produce insulin, although studies suggest that this damage may be reversible and is accompanied by an inability of the body to process insulin efficiently.

Historically, diagnosis of Diabetes Mellitus relied on measurements of blood glucose or fasting plasma glucose (FPG). Current recommendations by the American Diabetes Association prioritize the use of Hemoglobin A1c (HbA1c) as a marker for diagnosis because it provides a look at the glycemic landscape within the last period of complete red

blood cell turnover (~120 days in humans and ~45 days in C57BL/6 mice (Dholakia et al., 2015; Lew and Tiffert, 2017; Sherwani et al., 2016)). The percentage of HbA1c in the blood serum measures the non-enzymatic glycation of hemoglobin (Kahanovitz et al., 2017). Studies of HbA1c levels between sexes demonstrate that diabetic females tend to have a higher percentage of glycated cells although men tend to be more sensitive to the increased blood glucose at lower levels (Du et al., 2016; G. D. F et al., 2019). Using the control groups to define a normal range of HbA1c in C57BL/6J mice from each sex, it was observed that elevated blood glucose in STZ-treated mice resulted in an increase in HbA1c, the magnitude of which was greater in the males than in the females as

**Table 4**  
Estimated tissue-level mechanical data from 4-pt bending tests.

Stress-strain data	Male		p-Value	Female		p-Value
	Control	STZ		Control	STZ	
	(n = 15)	(n = 15)		(n = 15)	(n = 15)	
Yield stress (MPa)	197.19 ± 45.32	189.57 ± 34.54	0.628317	238.54 ± 47.08	191.17 ± 43.54	<b>0.003755</b>
Ultimate stress (MPa)	202.12 ± 43.3	194.52 ± 30.44	0.631602	244.48 ± 46.08	193.39 ± 45.12	<b>0.002014</b>
Strain to yield (mε)	22.88 ± 3.89	23.85 ± 5.93	0.583495	20.28 ± 4.62	20.51 ± 4.68	0.894482
Total strain (mε)	40.55 ± 19.54	36.23 ± 20.51	0.460959	28.07 ± 98.3	28.83 ± 15.28	0.902462
Resilience (MPa)	2.39 ± 0.59	2.42 ± 0.75	0.898884	2.59 ± 0.59	2.17 ± 0.77	0.098414
Toughness (MPa)	5.2 ± 3.07	3.8 ± 1.74	0.436289	4.15 ± 1.54	3.69 ± 2.97	0.097526
Elastic modulus (GPa)	9.74 ± 2.81	8.88 ± 2.01	0.136974	13.71 ± 4.41	10.48 ± 2.66	<b>0.020902</b>

Values in bold denote significance.

documented in humans (Chandramouli et al., 2018; Tramunt et al., 2020). Other work by our lab has shown that allowing the diabetic state to persist longer results in HbA1c levels as high as 14 % in diabetic female mice. This finding supports the idea that glycation will increase over time, potentially resulting in a more profound disease state with secondary complications.

It was hypothesized that one such complication of elevated blood glucose would be the presence of increased AGEs within the bone tissue which would lead to a stiffening of the collagen matrix (Meng et al., 2015). Neither an increase in AGEs (measured here using an assay specific to fluorescent AGEs) nor mechanical displacement or strain were altered here, but there are reasons why these data should not discount the hypothesis altogether. While an increase in glycated-hemoglobin exists within the sugar-saturated blood, increased glucose likely takes longer to infiltrate the interstitial fluid in the bone leading to an increase in bone AGEs. Future studies will include looking at the development of AGEs after longer exposure to glucose. Additionally, the most abundant AGEs in bone, such as methylglyoxal-derived hydroimidazolone (MG-H1) and carboxymethyl-lysine (CML) do not autofluoresce and therefore are not detected by a fluorescence assay. Future studies will also use ELISA tests which are reported to successfully quantify CML in bone samples to explore whether increased AGEs are present even in the absence of changes in mechanical deformation (Goh and Cooper, 2008; Sroga and Vashishth, 2021).

Diabetic mice were significantly smaller at the end of the study than their previously weight and sex matched control cohorts. In females, tibial length of the treated cohort was significantly shorter than the tibial length of the control cohort indicating an impact on longitudinal bone growth. This was mirrored in the reduction in both trabecular and cortical bone parameters which may also have contributed to the lower mass of the STZ-treated females.  $\mu$ CT revealed thinner trabeculae in STZ-treated animals of both sexes when compared with data from the control animals. A deficit was also observed in the cortical bone of STZ treated mice, but only in females. A lower bone area fraction was calculated for STZ-treated animals of both sexes, however, in males this was driven by an increase in marrow area with no change in total or bone area while in females the reduced bone area fraction was driven by a reduced bone area. This result in males was in keeping with previously reported data, although past papers did not provide enough data to compare the driving factors behind the change. This was also reflected in the significantly lower principal moments of inertia in the female-STZ bones. Trabecular TMD was lower in STZ-treated mice from both sexes, but cortical TMD was higher, reaching significance in STZ-treated males. In general, the mechanisms responsible for regulating TMD are not fully understood, and the reason for TMD being decreased in cancellous locations but increased in cortical bone sites in STZ-treated mice is not clear. In the future, attempts to monitor TMD longitudinally to determine when levels become differentially regulated, and to characterize the mineral's composition in the two bone compartments, may help to elucidate the nuances seen in these bones.

The deficit of published data on the mechanical performance of bone

in this mouse model makes it difficult to compare with other published studies. Much of the previous work reporting geometric changes to bone properties in rats and mice relied on histological evaluation, where our lab performed specific, quantitative measurement via microcomputed tomography with resolution of 9.8  $\mu$ m. Because of this, it is impossible to compare our numerical results with past reported data, even within the same mouse strain. Additionally, reported mechanical data relied on torsion testing, which cannot be directly equated to measures of strength in bending, and testing of femora in three-point bending, the results of which cannot be directly compared to results of four-point bending in tibiae. Absent a published report of the effects of STZ on the geometric or mechanical properties of primary bone formation in female C57Bl/6J mice, the decision was made to fully characterize the geometric and mechanical parameters of bone in both sexes.

From mechanical tests to failure, the strength (represented by the yield and maximum forces) of bones from STZ-treated females was significantly compromised. On average, the maximum load-carrying capacity of the STZ-treated females was 65 % that of control females. The nearly 40 % decrease in the stiffness of STZ-treated female bones reflects this decrease in strength as displacement values did not differ between groups. Although both sexes experienced a reduction in the amount of work to yield, the decrease in stiffness and strength did not reach significance in male mice. In STZ-female mice, changes in stress and elastic modulus reflect detrimental alterations to tissue quality. STZ-male had no significant differences in tissue-level mechanical properties, although trends were similar. Overall, the more compelling deficiencies in cortical geometry couple with decreased tissue-level mechanical behavior in the STZ-treated female mice drove the pronounced whole bone mechanical phenotype observed in these mice.

Although our results indicate this model is a suitable tool for future investigations of T1D in bone, this study is not without limitations. The differential dosing of the males and females prevents direct comparison that could be useful in understanding how the sexes respond differently to STZ and it is possible that the dose of STZ in males affected the HbA1c levels without being potent enough to affect the bone in the same manner as the females. While we showed that control mice modulated BG more effectively than STZ mice, the lack of a direct test for circulating levels of insulin limits our ability to understand the full effect of the BG on the insulin levels. Finally, the relatively short time period of this study limited exploration of the long-term effects of STZ on bone. This will be left to future work.

The successful induction of a Diabetes in both sexes using STZ was indicated by persistent high glucose in the blood, elevated HbA1c levels, and decreased architectural and mechanical properties of the bone. Female mice experienced altered mineral density in the bone, compromised bone quality, and reduced longitudinal growth in keeping with clinical diabetic outcomes (Sundararaghavan et al., 2017). The ability of this model to mimic human symptoms of diabetes, as well as the presentation of a strong bone disease phenotype, makes the STZ-induced diabetic mouse a suitable candidate for future work studying the impacts of diabetes in bone and potential therapeutics to ameliorate

observed bone alterations.

### CRedit authorship contribution statement

**Jennifer M. Hatch:** Conceptualization, Methodology, Validation, Formal analysis, Investigation, Writing – original draft, Writing – review & editing, Visualization. **Dyann M. Segvich:** Conceptualization, Validation, Formal analysis, Investigation. **Rachel Kohler:** Methodology, Validation, Formal analysis, Investigation. **Joseph M. Wallace:** Conceptualization, Formal analysis, Resources, Writing – review & editing, Supervision, Project administration, Funding acquisition.

### Declaration of competing interest

The authors declare that they have no known competing financial interests or personal relationships that could have appeared to influence the work reported in this paper.

### Acknowledgments

This work was supported by the National Institutes of Health (R01 AR072609 to JMW).

### References

- Bell, R.C., Khurana, M., Ryan, E.A., Finegood, D.T., 1994. Gender differences in the metabolic response to graded numbers of transplanted islets of langerhans. *Endocrinology* 135 (6), 2681–2687. <https://doi.org/10.1210/endo.135.6.7988458>. Dec.
- Bortolin, R.H., et al., 2015. Protection against T1DM-induced bone loss by zinc supplementation: biomechanical, histomorphometric, and molecular analyses in STZ-induced diabetic rats. *PLoS One* 10 (5), e0125349. <https://doi.org/10.1371/journal.pone.0125349>.
- Botolin, S., McCabe, L.R., 2007. Bone loss and increased bone adiposity in spontaneous and pharmacologically induced diabetic mice. *Endocrinology* 148 (1), 198–205. <https://doi.org/10.1210/en.2006-1006>. Jan.
- Bouillon, R., 1991. Diabetic bone disease. *Calcif. Tissue Int.* 49 (3), 155–160. <https://doi.org/10.1007/BF02556109>. Sep.
- Bouillon, R., 1992. Diabetic bone disease. Low turnover osteoporosis related to decreased IGF-I production [Online]. Available: *Verh K Acad Geneesk Belg* 54 (4), 365–391 <https://www.ncbi.nlm.nih.gov/pubmed/1466160>.
- Chandramouli, C., et al., 2018. Diastolic dysfunction is more apparent in STZ-induced diabetic female mice, despite less pronounced hyperglycemia. *Sci. Rep.* 8 (1), 2346. <https://doi.org/10.1038/s41598-018-20703-8>. Feb 5.
- Cignachi, N.P., et al., 2020. Bone regeneration in a mouse model of type 1 diabetes: influence of sex, vitamin D3, and insulin. *Life Sci.* 263, 118593. <https://doi.org/10.1016/j.lfs.2020.118593>. Dec 15.
- Cortright, R.N., Collins, H.L., Chandler, M.P., Lemon, P.W., DiCarlo, S.E., 1996. Diabetes reduces growth and body composition more in male than in female rats. *Physiol. Behav.* 60 (5), 1233–1238. [https://doi.org/10.1016/s0031-9384\(96\)00222-3](https://doi.org/10.1016/s0031-9384(96)00222-3). Nov.
- Dholakia, U., Bandyopadhyay, S., Hod, E.A., Prestia, K.A., Kevin A., 2015. Determination of RBC survival in C57BL/6 and C57BL/6-Tg (UBC-GFP) mice. *Comp. Med.* 65 (3), 5.
- Du, T., Yuan, G., Zhou, X., Sun, X., 2016. Sex differences in the effect of HbA1c-de fi ned diabetes on a wide range of cardiovascular disease risk factors. *Ann. Med.* 48 (1–2), 34–41. <https://doi.org/10.3109/07853890.2015.1127406>.
- Einhorn, T.A., Boskey, A.L., Gundberg, C.M., Vigorita, V.J., Devlin, V.J., Beyer, M.M., 1988. The mineral and mechanical properties of bone in chronic experimental diabetes. *J. Orthop. Res.* 6, 7.
- Fowlkes, J.L., et al., 2008. Runx-related transcription factor 2 (RUNX2) and RUNX2-related osteogenic genes are down-regulated throughout osteogenesis in type 1 diabetes mellitus. *Endocrinology* 149 (4), 1697–1704. <https://doi.org/10.1210/en.2007-1408>. Apr.
- G. D. F, et al., 2019. Sex differences and correlates of poor glycaemic control in type 2 diabetes: a cross-sectional study in Brazil and Venezuela. *BMJ Open* 9 (3), e023401. <https://doi.org/10.1136/bmjopen-2018-023401>. Mar 5.
- Goh, S.Y., Cooper, M.E., 2008. Clinical review: the role of advanced glycation end products in progression and complications of diabetes. *J. Clin. Endocrinol. Metab.* 93 (4), 1143–1152. <https://doi.org/10.1210/jc.2007-1817>. Apr.
- Gupte, A.A., Pownall, H.J., Hamilton, D.J., 2015. Estrogen: an emerging regulator of insulin action and mitochondrial function. *J. Diabetes Res.* 2015, 916585 <https://doi.org/10.1155/2015/916585>, 2015/03/26.
- Gurley, S.B., Clare, S.E., Snow, K.P., Hu, A., Meyer, T.W., Coffman, T.M., 2006. Impact of genetic background on nephropathy in diabetic mice. *Am. J. Physiol. Renal Physiol.* 290 (1), F214–F222. <https://doi.org/10.1152/ajprenal.00204.2005>. Jan.
- Hamada, Y., Kitazawa, S., Kitazawa, R., Fujii, H., Kasuga, M., Fukagawa, M., 2007. Histomorphometric analysis of diabetic osteopenia in streptozotocin-induced diabetic mice: a possible role of oxidative stress. *Bone* 40 (5), 1408–1414. <https://doi.org/10.1016/j.bone.2006.12.057>. May.
- Hayashi, K., Kojima, R., Ito, M., 2006. Strain differences in the diabetogenic activity of streptozotocin in mice. *Biol. Pharm. Bull.* 29 (6), 1110–1119. <https://doi.org/10.1248/bpb.29.1110>. Jun.
- Hie, M., Iitsuka, N., Otsuka, T., Tsukamoto, I., Sep 2011. Insulin-dependent diabetes mellitus decreases osteoblastogenesis associated with the inhibition of Wnt signaling through increased expression of Sost and Dkk1 and inhibition of Akt activation. *Int. J. Mol. Med.* 28 (3), 455–462. <https://doi.org/10.3892/ijmm.2011.697>.
- Horcajada-Molteni, M.N., et al., 2001. Amylin and bone metabolism in streptozotocin-induced diabetic rats. *J. Bone Miner. Res.* 16 (5), 958–965. <https://doi.org/10.1359/jbmr.2001.16.5.958>. May.
- Hough, F.S., Pierroz, D.D., Cooper, C., Ferrari, S.L., Bone, I.C., G. Diabetes Working, 2016. MECHANISMS IN ENDOCRINOLOGY: mechanisms and evaluation of bone fragility in type 1 diabetes mellitus. *Eur. J. Endocrinol.* 174 (4), R127–R138. <https://doi.org/10.1530/EJE-15-0820>. Apr.
- Inaba, M., et al., 1995. Influence of high glucose on 1,25-dihydroxyvitamin D3-induced effect on human osteoblast-like MG-63 cells. *J. Bone Miner. Res.* 10 (7), 1050–1056. <https://doi.org/10.1002/jbmr.5650100709>. Jul.
- Jeffcoate, W.J., Game, F., Cavanagh, P.R., 2005. The role of proinflammatory cytokines in the cause of neuropathic osteoarthropathy (acute charcot foot) in diabetes. *Lancet* 366 (9502), 2058–2061. [https://doi.org/10.1016/S0140-6736\(05\)67029-8](https://doi.org/10.1016/S0140-6736(05)67029-8).
- Jin, Y., et al., Sep 2013. The expression of inflammatory genes is upregulated in peripheral blood of patients with type 1 diabetes. *Diabetes Care* 36 (9), 2794–2802. <https://doi.org/10.2337/dc12-1986>.
- Junod, A., Lambert, A.E., Orci, L., Pictet, R., Gonet, A.E., Renold, A.E., 1967. Studies of the diabetogenic action of streptozotocin. *Proc. Soc. Exp. Biol. Med.* 126 (1), 201–205. <https://doi.org/10.3181/00379727-126-32401>. Oct.
- Kahanovitz, L., Sluss, P.M., Russell, S.J., 2017. Type 1 diabetes - a clinical perspective. *Point Care* 16 (1), 37–40. <https://doi.org/10.1097/POC.0000000000000125>. Mar.
- Kohler, R., et al., 2021. The effect of single versus group muCT on the detection of trabecular and cortical disease phenotypes in mouse bones. *J. Bone Miner. Res.* 36 (4), e10473. <https://doi.org/10.1002/jbmr.410473>. Apr.
- Le May, C., et al., 2006. Estrogens protect pancreatic B-cells from apoptosis and prevent insulin-deficient diabetes mellitus in mice. *PNAS* 103 (24), 6.
- Leiter, E.H., 1985. Differential susceptibility of BALB/c sublines to diabetes induction by multi-dose streptozotocin treatment. *Curr. Top. Microbiol. Immunol.* 122, 78–85. [https://doi.org/10.1007/978-3-642-70740-7\\_12](https://doi.org/10.1007/978-3-642-70740-7_12).
- Lew, V.L., Tiffert, T., 2017. On the mechanism of human red blood cell longevity: roles of calcium, the sodium pump, PIEZO1, and gards channels. *Front. Physiol.* 8, 977. <https://doi.org/10.3389/fphys.2017.00977>.
- Lu, H., Kraut, D., Gerstenfeld, L.C., Graves, D.T., 2003. Diabetes interferes with the bone formation by affecting the expression of transcription factors that regulate osteoblast differentiation. *Endocrinology* 144 (1), 346–352. <https://doi.org/10.1210/en.2002-220072>. Jan.
- Meng, H.Z., Zhang, W.L., Liu, F., Yang, M.W., 2015. Advanced glycation end products affect osteoblast proliferation and function by modulating autophagy via the receptor of advanced glycation end products/Raf protein/mitogen-activated protein kinase/extracellular signal-regulated kinase/extracellular signal-regulated kinase (RAGE/Raf/MEK/ERK) pathway. *J. Biol. Chem.* 290 (47), 28189–28199. <https://doi.org/10.1074/jbc.M115.669499>.
- Motyl, K., McCabe, L.R., 2009. Streptozotocin, type I diabetes severity and bone. *Biol. Proced. Online* 11, 296–315. <https://doi.org/10.1007/s12575-009-9000-5>.
- Nahdi, A.M.T.A., John, A., Raza, H., 2017. Elucidation of molecular mechanisms of streptozotocin-induced oxidative stress, apoptosis, and mitochondrial dysfunction in rin-5F pancreatic β-cells. *Oxidative Med. Cell. Longev.* 2017, 7054272 <https://doi.org/10.1155/2017/7054272>, 2017/08/06.
- Nakamura, M., Nagafuchi, S., Yamaguchi, K., Takaki, R., 1984. The role of thymic immunity and insulinitis in the development of streptozotocin-induced diabetes in mice. *Diabetes* 33 (9), 894–900. <https://doi.org/10.2337/diab.33.9.894>. Sep.
- Ndisang, J.F., Vannacci, A., Rastogi, S., 2017. Insulin resistance, type 1 and type 2 diabetes, and related complications 2017. *J. Diabetes Res.* 2017, 1478294 <https://doi.org/10.1155/2017/1478294>.
- Ni, L.H., et al., 2019. FK506 prevented bone loss in streptozotocin-induced diabetic rats via enhancing osteogenesis and inhibiting adipogenesis. *Ann. Transl. Med.* 7 (12), 265. <https://doi.org/10.21037/atm.2019.05.44>. Jun.
- Niu, S., et al., 2016. Broad infiltration of macrophages leads to a proinflammatory state in streptozotocin-induced hyperglycemic mice. *J. Immunol.* 197 (8), 3293–3301. <https://doi.org/10.4049/jimmunol.1502494>.
- Palta, M., LeCaire, T.J., Sadek-Badawi, M., Herrera, V.M., Danielson, K.K., 2014. The trajectory of IGF-1 across age and duration of type 1 diabetes. *Diabetes Metab. Res. Rev.* 30 (8), 777–783. <https://doi.org/10.1002/dmrr.2554>. Nov.
- Portal-Nunez, S., Lozano, D., de Castro, L.F., de Gortazar, A.R., Noguez, X., Esbrit, P., 2010. Alterations of the Wnt/beta-catenin pathway and its target genes for the N- and C-terminal domains of parathyroid hormone-related protein in bone from diabetic mice. *FEBS Lett.* 584 (14), 3095–3100. <https://doi.org/10.1016/j.febslet.2010.05.047>.
- National Diabetes Statistics Report 2020 Estimates of Diabetes and Its Burden in the United States [Online]. Available, 2020. United States Department of Health and Human Services Centers for Disease Control and Prevention <https://www.cdc.gov/diabetes/pdfs/data/statistics/national-diabetes-statistics-report.pdf>.
- Santana, R.B., Xu, L., Chase, H.B., Amar, S., Graves, D.T., Trackman, P.C., 2003. A role for advanced glycation end products in diminished bone healing in type 1 diabetes. *Diabetes* 52 (6), 1502–1510. <https://doi.org/10.2337/diabetes.52.6.1502>. Jun.
- Schwartz, A.V., et al., 2002. Older women with diabetes have a higher risk of falls: a prospective study. *Diabetes Care* 25 (10), 1749–1754. <https://doi.org/10.2337/diacare.25.10.1749>. Oct.

- Shaw, J.E., Sicree, R.A., Zimmet, P.Z., 2009. Global estimates of the prevalence of diabetes for 2010 and 2030. *Diabetes Res. Clin. Pract.* 87 (1), 10. <https://doi.org/10.1016/j.diabres.2009.10.007>, 11/9/2009.
- Sherwani, S.I., Khan, H.A., Ekhzaimy, A., Masood, A., Sakharkar, M.K., 2016. Significance of HbA1c test in diagnosis and prognosis of diabetic patients. *Biomark. Insights* 11, 95–104. <https://doi.org/10.4137/BMI.S38440>.
- Sroga, G.E., Vashishth, D., 2021. Controlled formation of carboxymethyllysine in bone matrix through designed glycation reaction. *JBMR Plus* 5 (11), e10548. <https://doi.org/10.1002/jbm4.10548>. Nov.
- Starup-Linde, J., Hygum, K., Harslof, T., Langdahl, B., 2019. Type 1 diabetes and bone fragility: links and risks. *Diabetes Metab. Syndr. Obes.* 12, 2539–2547. <https://doi.org/10.2147/DMSO.S191091>.
- Sundararaghavan, V., Mazur, M.M., Evans, B., Liu, J., Ebraheim, N.A., 2017. Diabetes and bone health: latest evidence and clinical implications. *Mar Ther. Adv. Musculoskelet. Dis.* 9 (3), 67–74. <https://doi.org/10.1177/1759720X16687480>. Mar.
- Tramunt, B., et al., 2020. Sex differences in metabolic regulation and diabetes susceptibility. *Diabetologia* 63 (3), 453–461. <https://doi.org/10.1007/s00125-019-05040-3>, 2020/03/01.
- Tsentidis, C., et al., 2016. Higher levels of s-RANKL and osteoprotegerin in children and adolescents with type 1 diabetes mellitus may indicate increased osteoclast signaling and predisposition to lower bone mass: a multivariate cross-sectional analysis. *Osteoporos. Int.* 27 (4), 1631–1643. <https://doi.org/10.1007/s00198-015-3422-5>. Apr.
- W. H. Organization, 2016. Global Report on Diabetes [Online]. Available: [http://apps.who.int/iris/bitstream/handle/10665/204871/9789241565257\\_eng.pdf;jsessionid=A8BA33D216173F7D351E7636BD84275B?sequence=1](http://apps.who.int/iris/bitstream/handle/10665/204871/9789241565257_eng.pdf;jsessionid=A8BA33D216173F7D351E7636BD84275B?sequence=1).
- Wallace, J.M., 2019. Skeletal hard tissue biomechanics. In: Burr, D.B., Allen, M.A. (Eds.), *Basic and Applied Bone Biology*, 2nd ed. Elsevier.
- Weinberg, E., Maymon, T., Moses, O., Weinreb, M., 2014. Streptozotocin-induced diabetes in rats diminishes the size of the osteoprogenitor pool in bone marrow. *Diabetes Res. Clin. Pract.* 103 (1), 35–41. <https://doi.org/10.1016/j.diabres.2013.11.015>. Jan.
- Yamagishi, S., Nakamura, K., Inoue, H., 2005. Possible participation of advanced glycation end products in the pathogenesis of osteoporosis in diabetic patients. *Med. Hypotheses* 65 (6), 1013–1015. <https://doi.org/10.1016/j.mehy.2005.07.017>.
- Zhao, Y.F., et al., 2013. Osteogenic potential of bone marrow stromal cells derived from streptozotocin-induced diabetic rats. *Int. J. Mol. Med.* 31 (3), 614–620. <https://doi.org/10.3892/ijmm.2013.1227>. Mar.
- Zhou, Z., et al., 2006. Regulation of osteoclast function and bone mass by RAGE. *J. Exp. Med.* 203 (4), 1067–1080. <https://doi.org/10.1084/jem.20051947>.
- [42] *Guide for the Care and Use of Laboratory Animals*, 2011. Institute for Laboratory Animal Research, Washington, D.C.